Supercooled vortex liquid and quantitative theory of melting of the flux-line lattice in type-II superconductors

Dingping Li[1,2] and Baruch Rosenstein[2,3]
[1]*Department of Physics, Peking University, Beijing 100871, China*
[2]*National Center for Theoretical Sciences and Electrophysics Department, National Chiao Tung University, Hsinchu 30050, Taiwan, Republic of China*
[3]*Department of Condensed Matter Physics, Weizmann Institute of Science, Rehovot 76100, Israel*
(Received 12 May 2003; revised manuscript received 10 May 2004; published 28 October 2004)

A metastable homogeneous state exists down to zero temperature in systems of repelling vortices. A zero-"fluctuation-temperature" liquid state therefore serves as a (pseudo) "fixed point" controlling the properties of vortex liquid below and even around melting point. Based on this picture for the vortex phase we apply the Borel-Pade resummation technique to develop a quantitative theory of the vortex liquid for the lowest-Landau-level Ginzburg-Landau model in type-II superconductors. While on the solid phase, there exists a superheat solid phase which ends at the spinodal line. The picture for the vortex phase is supported by an exactly solvable large N Ginzburg-Landau model in a magnetic field and has been recently confirmed by the experiments. The applicability of the lowest-Landau-level model is discussed and corrections due to higher levels are calculated. The melting line is located based on the quantitative theory for the description of the vortex solid and the vortex liquid. Magnetization, entropy, and specific heat jumps along the melting line are calculated. The theoretical results explain quantitatively very well the experimental data on the high-T_c cuprates $YBa_2Cu_3O_7$, DyBCO, low-T_c material (K, Ba) BiO_3, and also Monte Carlo simulation results.

DOI: 10.1103/PhysRevB.70.144521 PACS number(s): 74.25.−q, 74.40.+k, 74.25.Ha, 74.25.Dw

I. INTRODUCTION

Abrikosov flux lines (vortices) created by magnetic field in type-II superconductors strongly interact with each other, creating highly correlated configurations like the vortex lattice. In high-T_c cuprates thermal fluctuations at relatively large temperatures are strong enough to melt the lattice. Several remarkable experiments demonstrated that the vortex lattice melting in high-T_c superconductors is first order with magnetization jumps[1] and spikes in specific heat.[2] Magnetization and entropy jumps were measured using local Hall probes,[1] superconducting quantum interference device,[3,4] (SQUID), torque magnetometry,[5,6] and integrating the specific heat spike.[2,7] It was found that in addition to the spike there is also a jump in specific heat in $YBa_2Cu_3O_7$ (YBCO) which was measured as well.[2,7,8] These precise measurements pose the question of an accurate quantitative theoretical description of thermal fluctuations in vortex matter.

The melting line in high-T_c cuprates has been studied mainly not very far from T_c. In this part of the phase diagram the Ginzburg-Landau (GL) approach is generally appropriate to describe thermal fluctuations near T_c.[9,10] The GL model is, however, highly nontrivial even within the lowest-Landau-level (LLL) approximation valid at relatively high fields. This simplified model has only one parameter: the dimensionless LLL scaled temperature $a_T \sim [T-T_{mf}(H)]/(TH)^{2/3}$ [defined precisely in Eq. (13) below]. Over the last 20 years a great variety of theoretical methods were applied to study this model. Brezin, Nelson, and Thiaville[11] applied the renormalization group (RG) method to the one-loop-level description of the vortex liquid. No nontrivial fixed points of the (functional) RG equations were found and they concluded therefore that the transition from liquid to solid is first order.[12] Another often-used approach applicable also beyond the range of validity of the GL model is to use an elasticity theory description of the vortex lattice and Lindermann criterion to determine the location of melting line.[13] However, all those approaches do not provide a quantitative theory of melting since these are one-phase theories and in order, for example, to calculate discontinuities at first-order transitions an accurate description of both phases is necessary.

Two perturbative approaches were developed and greatly improved recently to describe both the solid and liquid phases in the LLL GL model. The perturbative approach on the liquid side was pioneered long ago by Ruggeri and Thouless.[14] They developed a perturbative expansion around a homogeneous (liquid) state in which all the "bubble" diagrams are resumed. Unfortunately they found that the series are asymptotic, and although a first few terms provide accurate results at very high temperatures, the series becomes inapplicable for a_T less than −2, which is quite far above the melting line (believed to be located around $a_T \sim -10$). We recently obtained an optimized Gaussian series[15] which is convergent rather than asymptotic with radius of convergence of $a_T=-5$, but it is still unfortunately above the melting point.

For the vortex solid in the LLL GL mode, Eilenberger[16] and Maki and Takayama[16] calculated the fluctuations spectrum around Abrikosov's mean-field solution. They noticed that the vortex lattice phonon modes are softer than that of the acoustic phonons in atomic crystals and this leads to infrared (IR) divergences in certain quantities. This was initially interpreted as the "destruction of the vortex solid by thermal fluctuations" and the perturbation theory was abandoned. However, the divergences look suspiciously similar to "spurious" IR divergences in the critical phenomenon theory

and recently it was shown that all these IR divergences cancel in the perturbative series for physical quantities, in particular the effective free energy.[17] The perturbative series therefore is reliable and was extended to two loops for the free energy. The free energy calculated to two loops on the solid side is now precise enough even around the melting point.

Therefore the missing part is a theory in the region $-10<a_T<-5$ for the liquid phase. Moreover, this theory should be very precise since free energies of solid and liquid happen to differ only by a few percent around melting. Closely related to melting is the problem of the nature of the metastable phases of the theory. While it is clear that the overheated solid becomes unstable at some finite temperature, it is not generally clear whether the overcooled liquid in the LLL GL model becomes unstable at some finite temperature (like water and other molecular liquids, which, however, have a crucial attractive component of the intermolecular force) or exists all the way down to $T=0$ as a metastable state. The Gaussian (Hartree-Fock) variational calculation, although perhaps of a limited precision, is usually a very good guide as far as the qualitative features of the phase diagram are concerned. Such a calculation in the liquid was performed long ago,[14] while a significantly more complicated one sampling also inhomogeneous states (vortex lattice) was obtained recently.[18,19] The Gaussian results are as follows. The free energy of the solid state is lower than that of the liquid for all temperatures lower than melting temperature a_T^m. The solid state is therefore the stable one below a_T^m, becomes metastable at somewhat higher temperatures, and is destabilized at $a_T=-5.5$. The liquid state becomes metastable below the melting temperature, but unlike the solid, does not lose metastability all the way down to $a_T^m=-\infty$ $(T=0)$. The excitation energy of the supercooled liquid approaches zero as a power $\varepsilon\sim 1/a_T^2$. This general picture is supported in Sec. III by an exactly solvable large N Ginzburg-Landau model of vortex matter in type-II superconductors.

In the meantime similar qualitative results were obtained in different area of physics. It was shown by variety of analytical and numerical methods that liquid (gas) phase of the classical one component Coulomb plasma exists as a metastable state down to very low temperature, possibly $T=0$.[20] The quantum one-component plasma-electron gas also shows similar features.[21] It seems plausible to speculate that the same phenomenon would happen in any system of pointlike or linelike objects interacting via purely repulsive forces. In fact the vortices in the London approximation are a sort of repelling lines with the force even more long range than Coulombic. This was an additional strong motivation to consider the above scenario in vortex matter. In addition to the above-mentioned theoretical evidence for the validity of the scenario, very recently, the supercooled vortex liquid at very low temperature and the superheat vortex solid which vanishes at spinodal line have been observed in a beautiful experiment on 2H-$NbSe_2$ by Xiao *et al.*[22] Previous experiments[23] showed that the observed effect is not due to surface pinning or geometrical barriers.

Assuming the absence of singularities on the liquid branch allows us develop an essentially precise theory of the LLL GL model for vortex liquid (even including supercooled liquid) using methods of theory of critical phenomena.[24,25] The generally effective mathematical tool to approach a nontrivial fixed point (in our case at zero temperature) is the Borel-Pade (BP) transformation.[25] Before embarking on this program in the following sections, we address several subtleties which prevented the use and acceptance of the BP method in the past. Very early on Ruggeri and Thouless[14] tried to use BP (unfortunately a "constrained" one, so that it interpolates smoothly with the solid, an assumption we believe is incorrect) to calculate the specific heat without much success. It was shown by Wilkin and Moore[26] that the constrained BP does not converge, while the results for unconstrained BP were inconclusive. They attributed this to the limited order of expansion known at that time. The BP liquid theory combining with the recently developed LLL theory of solids could be used to calculate the melting line and the magnetization and the specific heat jumps across the line.[27] The attempts to use BP for the calculation of the melting line using a longer series also ran into problems. Hikami, Fujita, and Larkin[27] tried to find the melting point by comparing the BP liquid free energy with the one-loop solid free energy and obtained $a_T=-7$. However, their one-loop solid energy was incorrect and, in any case, it was not precise enough (as will become clear in the following discussions that the two-loop contribution cannot be neglected).

The LLL GL model has been studied by various methods. For example, it was also studied numerically in both the Lawrence-Doniach model [a good approximation of the three-dimensional (3D) GL for large number of layers] (Refs. 28 and 29) and in 2D (Ref. 30) and by a variety of nonperturbative analytical methods, among them the density functional,[31] $1/N$,[32–34] dislocation theory of melting,[35] and others.[36] However, most of those theories in the literature are qualitative and have not given us a quantitative description (locations of melting lines, magnetization jumps, entropy jumps, etc.) for the melting of vortex lattice. The theory we will describe in this article can face the experimental test and we found that the predication and results from the theory is in good quantitative agreement with experiments.

As we show in this paper, the BP liquid free energy combined with the correct two-loop solid energy computed recently gives scaled melting temperature $a_T^m=-9.5$ and in addition predicts other characteristics of the model. The magnetization of liquid is larger than that of solid by approximate 1.8% irrespective of the melting temperature (the specific heat jump is about 6% and decreases slowly with temperature in YBCO). A brief account of these results was published.[18]

In addition to the theory of melting, we considered overcooled liquid and calculated magnetization and specific heat curves. Since the metastable overcooled liquid state exists all the way down to zero temperature in the model, we can define the liquid Madelung energy. Looking at the melting process from the low-temperature side for both the liquid and solid we find that the Madelung energy of the liquid is larger than that of the solid approximately by the latent heat of melting. Our magnetization curves agree quite well with Monte Carlo simulations of the LLL GL (Ref. 28) and almost perfectly for the specific heat in 2D by Kato and Nagaosa in Ref. 30.

We study also in this paper several "phenomenological" issues, some matter of significant disagreement. First is the range of applicability of the LLL model. We find that in order to describe the experimental reversible magnetization of YBCO at lower fields, higher-Landau-levels (HLL) corrections should be incorporated. We therefore clarify in Sec. V the role of the HLL modes. Experimentally it was claimed that one can establish the LLL scaling for fields above $3T$.[37] A glance at the data, however, shows that in normal state (above T_c) the LLL scaling for magnetization curves is generally very bad. Most of the HLL effects can be taken into account by just renormalizing the parameters of the LLL model. Therefore one should use the "effective LLL" in which HLL were "integrated out." To clarify this oftensalient feature we explicitly perform this integration within a self-consistent approach in Sec. V. It was noted by Koshelev[38] and others that, to calculate magnetization, one has to carefully account for renormalization of the free energy since it is field dependent. Then we calculated the leading correction to the effective LLL and compare it with experiments. It is found that although the LLL contribution to magnetization is much larger that the experimentally observed one above T_c, it is nearly canceled by the HLL contributions. This explains the breaking of the LLL scaling in the normal state.

The paper is organized as follows. The model is defined and its applicability range discussed in Sec. II. In Sec. III, the (including supercooled) liquid and (including superheated) solid in the LLL GL will be discussed in the mean-field approximation of the LLL GL model and in the large-N LLL GL model. In Sec. IV, the LLL model is solved and the melting theory of vortex lattice is presented and compared to experiments. In Sec. V, the HLL corrections are discussed and the magnetization curves are compared with experiments.

In particular phenomenological issues are addressed in Secs. II B (assumptions), IV C (melting line, Ginzburg parameter fit for various materials), IV D (magnetization, entropy jumps), IV E (specific heat jumps), and V D (reversible magnetization curve), so readers not interested in theoretical details can go directly to these sections.

II. GL MODEL AND ITS BASIC ASSUMPTIONS

A. GL model

On the mesoscopic scale, 3D superconducting materials, with not very strong asymmetry along the z axis which we call as YBCO-type superconductors, are effectively described by the Ginzburg-Landau free energy functional

$$F[\psi,\psi^*,\mathbf{A}]=\int d^3x\frac{\hbar^2}{2m_{ab}}|\mathbf{D}\psi|^2+\frac{\hbar^2}{2m_c}|\partial_z\psi|^2-a(T)|\psi|^2+\frac{b'}{2}|\psi|^4+\frac{(\mathbf{B}-\mathbf{H})^2}{8\pi} \quad (1)$$

involving the order parameter field ψ and magnetic field $\mathbf{B}$. The external constant magnetic field is described by the vector potential in Landau gauge $\mathbf{A}_0=(Hy,0,0)$. The covariant derivative is defined by $\mathbf{D}\equiv\boldsymbol{\nabla}-2\pi i\mathbf{A}/\boldsymbol{\Phi}_0,\Phi_0\equiv hc/e^*$ ($e^*=2e$). The microscopic thermal fluctuations are integrated out and, as a consequence, coefficients a, b', and m depend on temperature. Mesoscopic thermal fluctuations of the order parameter are described by the partition function

$$Z=\int\mathcal{D}\psi\mathcal{D}\psi^*\,\mathcal{D}\mathbf{A}\exp\left\{-\frac{F[\psi,\psi^*,\mathbf{A}]}{T}\right\}. \quad (2)$$

Our aim is to quantitatively describe the effects of thermal fluctuations of high-T_c cuprates of the YBCO type.

B. Assumptions

The use of the above GL free energy hinges upon several physical assumptions. They are listed below.

(i) *Continuum 3D model*. We use the anisotropic GL model despite the well established layered structure of the high T_c cuprates for which models of the Lawrence-Doniach type are more appropriate. Effects of layered structure are dominant in BSCCO or Tl compounds (anisotropy very large: $\gamma\equiv\sqrt{m_c/m_{ab}}>1000$) and noticeable for cuprates with anisotropy of order $\gamma=50$ like LaBaCuO, strongly underdoped YBCO (see, however, Ref. 39), or Hg1223. The requirement that the 3D GL model can be effectively used therefore limits us to optimally doped $YBCO_{7-\delta}$ (or slightly overdoped or underdoped) for which the anisotropy parameter is not very large [around $\gamma=4-8$ (Ref. 40)], DyBCO and possibly Hg1221 which has a slightly larger anisotropy. However there is no such problem in recently discovered isotropic "fluctuating" superconductor (K, Ba) BiO_3.[41]

(ii) *Range of validity of the mesoscopic (GL) approach*. The GL approach generally is an effective mesoscopic approach. It is applicable when one can neglect higher-order terms in the functional of Eq. (1), typically generated when one "integrates out" microscopic degrees of freedom. The leading higher-dimensional terms we neglect (as "irrelevant") are $|\psi|^6$ and higher (four) derivative terms like $|\mathbf{D}^2\psi|^2$. This naively leads to a condition that $1-t-b$ is smaller than 1. Here and in what follows, one defines

$$t\equiv T/T_c,\quad b\equiv B/H_{c2}\approx H/H_{c2}\equiv h. \quad (3)$$

The applicability line $1-t-b<0.2$ for YBCO is plotted in Fig. 1. We also will consider a model invariant under rotations in the ab plane. Noninvariant models sometimes can be rescaled to $m_a\simeq m_b=m_{ab}$.[10]. For several physical questions those assumptions are not valid because neglected "irrelevant" terms might become "dangerous." For example the question of the structural phase transition into the square lattice is clearly of this type.[42] It is known that even assuming $m_a/m_b=1$ in low-temperature vortex lattices in YBCO, rotational symmetry is broken down to the fourfold symmetry by the four derivative terms. However, there is no significant correction to other physical quantities—for example, the magnetization from those higher-dimensional terms.

(iii) *Expansion of parameters around T_c*. Generally the parameters of the GL model of Eq. (1) are complicated functions of temperature which are determined by the details of the microscopic theory. We expand the coefficient $a(T)$ near T_c:

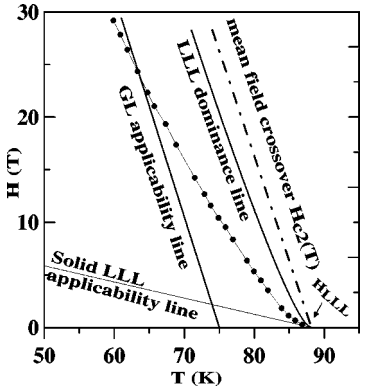

FIG. 1. Comparison of the experimental melting line for fully oxidized $YBa_2Cu_3O_7$ Ref. 6 with our theoretical fitting. Applicability of the LLL approximation is between two lines, the solid LLL applicability line and the (liquid) LLL dominance line. The GL model applicability line is also plotted.

$$a(T) = T_c[\alpha(1-t) - \alpha'(1-t)^2 + \cdots]. \tag{4}$$

The second and higher terms in the expansion are omitted and therefore, when temperature deviates significantly from T_c, one cannot expect the model to have a good precision. We note that recently measured $H_{c2}(T)$ is linear in T in a wide region near T_c in both YBCO and $(K,Ba)BiO_3$.[41,43]

(iv) *Constant nonfluctuating magnetic field*. For strongly type-II superconductors like the high-T_c cuprates not very far from $H_{c2}(T)$ (this easily covers the range of interest in this paper; for the detailed discussion of the range of applicability beyond it see Ref. 44), the magnetic field is homogeneous to a high degree due to superposition from many vortices. Inhomogeneity is of order $1/\kappa^2 \sim 10^{-3}$. Since the main subject of this study is thermal fluctuation effects of the order parameter field, one might ask whether thermal fluctuations of the electromagnetic field should be also taken into account. Halperin, Lubensky, and Ma considered this question long time ago.[45] The conclusion was that they are completely negligible for very large κ. Upon discovery of the high-T_c cuprates, the issue was reconsidered[46] and the same result was obtained to a very high precision. Therefore here magnetic field is treated both as constant and nonfluctuating ($B=H$) and the last term in Eq. (1) can be omitted (to precision of order $1/\kappa^2$). However, when we calculate the magnetization $M=(B-H)/4\pi$, which is of order $1/\kappa^2$, a higher-order correction must be considered.

Recently it was claimed that the "vortex loop" fluctuations are important and even might lead to additional phase transition at field of order Gi H_{c2}.[47] This is of order 100 G for the materials of interest listed in Table II and therefore is irrelevant for physics discussed in this paper. Note that Gi in the papers discussing the vortex loops physics[48] is assumed to be much larger. We discuss this issue in Sec. IV C.

(v) *Disorder*. Point like disorder is always present in Y BCO. For example magnetization becomes irreversible. The melting line of the optimally doped or underdoped samples bends towards lower fields[7] and signs of the second-order transition appear at $12T$.[49] However, in some samples like fully oxidized $YBa_2Cu_3O_7$ (Ref. 6) and $DyBa_2Cu_3O_7$ (Refs. 8 and 50) the disorder effects are minor especially at temperature close to T_c. In the maximally oxidized YBCO,[6] the second-order transition associated with disorder is not seen even at the highest available fields (30 T). Certain aspects of the disorder problem were addressed in the framework of GL theory,[51] elasticity theory,[52] and a phenomenological approach based on the Lindermann criterion.[13]

Throughout the most of the paper, we will use the coherence length $\xi=\sqrt{\hbar^2/(2m_{ab}\alpha T_c)}$ as a unit of length, T_c as unit of temperature, and $[dH_{c2}(T_c)/dT]T_c=\Phi_0/2\pi\xi^2$ as a unit of magnetic field. As we mentioned above, we assume constant magnetic induction $\mathbf{B}=\mathbf{b}H_{c2}$ which is slightly different from the external magnetic field $\mathbf{H}=\mathbf{h}H_{c2}$. After rescaling Eq. (1) by $x\to\xi x$, $y\to\xi y$, $z\to\xi z/\gamma$, and $\psi^2\to(2\alpha T_c/b')\psi^2$ ($\gamma\equiv\sqrt{m_c/m_{ab}}$) one obtains the Boltzmann factor

$$f = \frac{F}{T} = \frac{1}{\omega}\int d^3x\left[\frac{1}{2}|\mathbf{D}\psi|^2 + \frac{1}{2}|\partial_z\psi|^2 - \left(a_h + \frac{b}{2}\right)|\psi|^2 + \frac{1}{2}|\psi|^4 + \frac{\kappa^2(\mathbf{b}-\mathbf{h})^2}{4}\right], \tag{5}$$

where the dimensionless parameter

$$\omega = \sqrt{2N_{\mathrm{Gi}}}\pi^2 t \tag{6}$$

characterizes the strength of thermal fluctuations and the rescaled $\mathbf{D}\equiv\boldsymbol{\nabla}-i\mathbf{A}$ with $\mathbf{A}=(by,0,0)$. The commonly used dimensionless Ginzburg number is defined by

$$N_{\mathrm{Gi}} \equiv \frac{1}{2}\left(\frac{32\pi e^2\kappa^2\xi T_c\gamma}{c^2h^2}\right)^2. \tag{7}$$

And

$$a_h = \frac{1-t-b}{2}. \tag{8}$$

defines the distance from the mean-field transition line.

C. Landau level modes in the quasimomentum basis

Assuming that all the requirements are met, we now divide the fluctuations into the LLL and HLL modes to make the problem manageable. It is convenient to expand the order parameter field in a complete basis of noninteracting theory: the Landau levels. In the hexagonal lattice phase the most convenient basis is the quasimomentum basis

$$\psi(x,y,z) = \frac{1}{\sqrt{2}(2\pi)^{3/2}}\int_k \sum_{n=0}^{\infty} e^{-ik_z z}\varphi_{\mathbf{k}}^n(x,y)\psi^n(\mathbf{k},k_z). \tag{9}$$

Here $\varphi_{\mathbf{k}}^n(x)$ is the eigenstate of the nth Landau level $\varepsilon_n=(n+1/2)b\left[\frac{1}{2}|\mathbf{D}\psi|^2\varphi_{\mathbf{k}}^n(x)=(n+1/2)b\varphi_{\mathbf{k}}^n(x)\right]$ with two-dimensional quasimomentum $\mathbf{k}$ with hexagonal symmetry:

$$\varphi_{\mathbf{k}}^{n}=\sqrt{\frac{\sqrt{\pi}}{2^{n-1}n!a_{\Delta}}}\sum_{l=-\infty}^{\infty}H_n\left(y\sqrt{b}+\frac{k_x}{\sqrt{b}}-\frac{2\pi}{a_{\Delta}}l\right)\times\exp\left\{i\left[\frac{\pi l(l-1)}{2}+\frac{2\pi(\sqrt{b}x-k_y/\sqrt{b})}{a_{\Delta}}l-xk_x\right]-\frac{1}{2}\left(y\sqrt{b}+\frac{k_x}{\sqrt{b}}-\frac{2\pi}{a_{\Delta}}l\right)^2\right\},\tag{10}$$

where $a_{\Delta}\equiv\sqrt{4\pi/\sqrt{3}}$. The function $\varphi_A\equiv\varphi_{\mathbf{k}=0}^{n=0}$ describes the Abrikosov lattice solution.[9] Even in the liquid state, which is more symmetric than the hexagonal lattice, we find it convenient to use this basis.

Naively, if the magnetic field is sufficiently high, the energy gap of the order b separating the $n=0$ LLL modes from the HLL is very large and it is reasonable to keep only the LLL modes in Eq. (5). The dominance of the LLL modes for melting was discussed in Ref. 11 and Pierson and Valls in Ref. 37, and we will discuss it in more detail in Sec. V. In the rest of this section, we consider the LLL GL model.

D. LLL scaling

Using the LLL condition $|\mathbf{D}\psi|^2=b|\psi|^2$, the free energy is simplified:

$$f=\frac{1}{\omega}\int d^3x\left[\frac{1}{2}|\partial_z\psi|^2-a_h|\psi|^2+\frac{1}{2}|\psi|^4+\frac{\kappa^2(\mathbf{b}-\mathbf{h})^2}{4}\right].\tag{11}$$

There is no longer a gradient term in directions perpendicular to the field and consequently the model possesses the LLL scaling.[53] After additional rescaling $x\to x/\sqrt{b}$, $y\to y/\sqrt{b}$, $z\to z(b\omega/4\pi\sqrt{2})^{-1/3}$, and $\psi\to(b\omega/4\pi\sqrt{2})^{1/3}\psi$, the dimensionless free energy takes the form

$$f=\frac{1}{4\pi\sqrt{2}}\int d^3x\left[\frac{1}{2}|\partial_z\psi|^2+a_T|\psi|^2+\frac{1}{2}|\psi|^4+\kappa^2\left(\frac{b\omega}{4\pi\sqrt{2}}\right)^{-4/3}\frac{(\mathbf{b}-\mathbf{h})^2}{4}\right].\tag{12}$$

Minimizing it with respect to b leads to magnetization $b-h$ of the order of $1/\kappa^2$. This means that in the strongly type-II limit ($\kappa\gg1$) the last term is of the order $1/\kappa^2$ and can be neglected. The theory has a single dimensionless parameter, the Thouless scaled temperature defined by

$$a_T=-\left(\frac{b\omega}{2^{5/2}\pi}\right)^{-2/3}a_h.\tag{13}$$

The Gibbs free energy density in the newly scaled model is defined as

$$g(a_T)=-\frac{4\pi\sqrt{2}}{V}\log\int D\psi D\psi^*\exp\{-f[\psi]\},\tag{14}$$

which is also a function of a_T only ($4\pi\sqrt{2}$ is the scaled "temperature"). The relation to the original Gibbs free energy is

$$G(T,H)=\frac{H_{c2}^2}{2\pi\kappa^2}\left(\frac{b\omega}{2^{5/2}\pi}\right)^{4/3}g(a_T).\tag{15}$$

III. OVERCOOLED LIQUID AND THE T=0 FIXED POINT OF THE LLL MODEL

In this section, we will show that in the mean-field approximation and the exact solvable large-N model, there is a zero-temperature pseudocritical point for the vortex liquid and the melting is a first-order phase transition. Moreover, there exists a superheat solid which ends at spinodal line.

The energy of the hexagonal solid in the mean field (neglecting mesoscopic thermal fluctuations) is[9]

$$g_M^{sol}=-\frac{a_T^2}{2\beta_A},\quad G_M^{sol}=-\frac{H_{c2}^2}{4\pi\kappa^2\beta_A}a_h^2,\tag{16}$$

where $\beta_A=1.1596$ and the subscript M underlies the similarity to the Madelung energy of atomic solids. The major fluctuations contribution to the solid free energy is due to the "phonon" modes. In harmonic approximation it is proportional to the fluctuation temperature $T=a_T^{-3/2}$:

$$g_1^{sol}=2.848|a_T|^{1/2},\quad G_1^{sol}=C_1^{sol}T,\tag{17}$$

$$C_1^{sol}=2.848\frac{H_{c2}B}{8\kappa^2T_c}\sqrt{|a_h|}.$$

At low fluctuation temperatures one can neglect the T dependence of $a_h\simeq-(1-b)/2$. The solid becomes unstable at $a_T=-5.5$ according to the self-consistent (Gaussian) approximation.[19]

In the (homogeneous) liquid state the order parameter vanishes and the contributions to the free energy come solely from fluctuations. The Gaussian ("mean-field") approximation to the free energy[14] is

$$g=4\sqrt{\varepsilon}-4/\varepsilon,\tag{18}$$

where the excitation energy ε is given by a solution of the cubic "gap equation"

$$\varepsilon^{3/2}-a_T\sqrt{\varepsilon}-4=0.\tag{19}$$

The liquid state becomes metastable below the melting temperature, but unlike the solid above melting, does not lose metastability at a certain "spinodal" point.[54] It persists all the way down to $T=0$. The excitation energy of the supercooled liquid approaches zero as a power $\varepsilon\sim16/a_T^2$. For $a_T\to-\infty$, the scaled energy, Eq. (18), has an expansion in $1/a_T^3\propto T^2$ for small fluctuation temperature T (the radius of convergency of the expansion extending to $a_T=-3$). Therefore the liquid despite having energy larger than that of the solid becomes (pseudo)critical[55] at zero temperature. Physical quantities "around" this point exhibit a power behavior with characteristic (pseudo)critical exponents. The metastable liquid state has a distinct Madelung energy

$$g_M^{liq}=-\frac{a_T^2}{4},\quad G_M^{liq}=-\frac{H_{c2}^2}{8\pi\kappa^2}a_h^2.\tag{20}$$

As the temperature increases the difference between the solid and liquid becomes smaller and vanishes at melting. Generally one expects a linear correction at small T:

$$G^{liq} = G_M^{liq} + C_1^{liq} T. \tag{21}$$

Since the expansion of the mean-field free energy is in T^2, $C_1^{liq}=0$. Comparing the solid free energy, Eqs. (16) and (17), with Eq. (21), we get the melting temperature $a_T^m=-6.3$. We therefore conclude that in this approximation the supercooled liquid state exists down to its pseudocritical point at zero temperature. Moreover, the pseudocritical point might govern the behavior of the liquid phase to temperatures as high as the melting point and there exists a good low-temperature expansion (stronger coupling expansion) for the supercooled liquid.

It is important to confirm the above scenario in an exactly solvable model. The simplest model of this kind is the multicomponent GL model. The LLL GL theory can be generalized (in several different ways) to an N-component order parameter field ψ^a, $a=1,\ldots,N$:

$$f = \frac{1}{4\pi\sqrt{2}} \int d^3x \left[\frac{1}{2}|\partial_z \psi^a|^2 + a_T|\psi^a|^2 + \frac{\nu}{2N}|\psi^a|^2|\psi^b|^2 + \frac{1-\nu}{2N}\psi^a\psi^a\psi^{*b}\psi^{*b} \right]. \tag{22}$$

The large-N limit of this theory can be solved in a way similar to that in the N-component scalar models widely used in theory of critical phenomena.[24] The simplest case $\nu=1$ has been considered in Ref. 32. It was found that the homogeneous state is stable at all temperatures. Under assumption that the conventional Abrikosov lattice takes over at low temperatures it supported the original conjecture by Brezin *et al.*[11] that melting of the flux lattice is a first-order phase transition. However, it was shown (by explicit numerical evaluation) in Ref. 12 that the low-temperature ground state in that model is not the Abrikosov lattice state in which just one component has a nonzero expectation value (similar to the one component Abrikosov lattice). The "true" ground state has infinite degeneracy. Different ground states at large N are markedly different from the hexagonal lattice. The case $\nu=2$, in which the Abrikosov lattice state is a stable ground state, was first introduced in Ref. 34 and we will refer it as the Lopatin-Kotliar (LK) model. Equation (22) is a slight generalization including both models studied in Refs. 32 and 34. We find that in fact all models with $\nu \geqslant 2$ possess such a stable lattice state.

A straightforward method to develop the $1/N$ expansion with the last component of ψ^N having the expectation value $\propto \varphi_A \equiv \varphi_{\mathbf{k}=0}^{n=0}$, describing the hexagonal lattice [see Eq. (10)], is to shift this field $\psi^N(x,y,z) \to \psi^N(x,y,z) + \sqrt{N} c \varphi_A(x,y)$, where c is a (real) constant. Then one introduces Hubbard-Stratonovich (HS) fields ρ, χ (Ref. 34) via free energy $f[\psi^a,\rho,\chi]$ equal to

$$\frac{1}{4\pi\sqrt{2}} \left\langle \frac{1}{2}|\partial_z\psi^a|^2 + (\nu\rho + a_T)|\psi^a|^2 + \nu c^2|\varphi_A|^2|\psi^a|^2 + \frac{1-\nu}{2}[(c^2\varphi_A^2 + \chi)\psi^{*b}\psi^{*b} + \text{c.c.}] \right\rangle_x - \frac{N}{4\pi\sqrt{2}} \left\langle \frac{\nu}{2}\rho^2 + \frac{1-\nu}{2}|\chi|^2 \right\rangle_x + N f_{nf} + \cdots. \tag{23}$$

Here the "nonfluctuating part" is the Abrikosov free energy density

$$f_{nf} = \frac{1}{4\pi\sqrt{2}} \left[a_T c^2 + \frac{\beta_A}{2} c^4 \right]. \tag{24}$$

We omitted several cubic terms which do not influence the leading order in $1/N$. Integrating over the fluctuating the ψ^a fields one obtains the effective scaled Gibbs energy density (the calculation is very similar to that in Ref. 19, where technical details can be found)

$$\frac{g_{\text{eff}}}{N} = a_T c^2 + \frac{\beta_A}{2} c^4 - \left\langle \frac{\nu}{2}\rho^2 + \frac{1-\nu}{2}|\chi|^2 \right\rangle_x + 2\left\langle \sqrt{\epsilon_O(\mathbf{k})} + \sqrt{\epsilon_A(\mathbf{k})} \right\rangle_{\mathbf{k}}. \tag{25}$$

The spectrum has two branches

$$\epsilon_{O,A}(\mathbf{k}) = a_T + \nu(\beta_k c^2 + \rho_k) \pm |(1-\nu)(c^2\gamma_k + \chi_k)|. \tag{26}$$

To have a stable *perturbative* Abrikosov solution which shall be a good solution for the low temperature, the spectrum should be positive definite for $\rho_k=\chi_k=0$ (in the *perturbative approach*, $\rho_k=\chi_k=0$ and $c^2=|a_T|/\beta_A$). Thus we demand $-\nu/2+(\nu-1)\geqslant 0$ or $\nu \geqslant 2$, as stated above.

The HS fields

$$\rho_k = \langle \rho(x)|\varphi_k(x)|^2\rangle_x, \quad \chi_k = \langle \chi(x)\varphi_k^*(x)\varphi_{-k}^*(x)\rangle_x, \tag{27}$$

and the constant c are determined by minimizing free energy g_{eff}.

Now we will study the inhomogeneous (solid) solution. The minimization with respect to $\rho(x)$ and $\chi(x)$ leads to

$$\rho(x) = \langle |\varphi_k(x)|^2 \{ [\epsilon_O(\mathbf{k})]^{-1/2} + [\epsilon_A(\mathbf{k})]^{-1/2} \} \rangle_k$$

$$\text{sgn}(1-\nu)\chi(x) = \left\langle \varphi_k(x)\varphi_{-k}(x) \frac{c^2\gamma_k + \chi_k}{|c^2\gamma_k + \chi_k|} \{ [\epsilon_O(\mathbf{k})]^{-1/2} - [\varepsilon_A(\mathbf{k})]^{-1/2} \} \right\rangle_k, \tag{28}$$

which, in terms of Fourier harmonics of the hexagonal lattice, takes a form

$$\rho_l = \langle \beta_{l-k} \{ [\epsilon_O(\mathbf{k})]^{-1/2} + [\epsilon_A(\mathbf{k})]^{-1/2} \} \rangle_k$$

$$\text{sgn}(1-\nu)\chi_l = \left\langle \gamma_{k,l}^* \frac{c^2\gamma_k + \chi_k}{|c^2\gamma_k + \chi_k|} \{ [\epsilon_O(\mathbf{k})]^{-1/2} - [\epsilon_A(\mathbf{k})]^{-1/2} \} \right\rangle_k. \tag{29}$$

The lattice functions β_k, γ_k, and $\gamma_{k,l}$ are defined as

$$\beta_k = \langle |\varphi|^2 \varphi_{\vec{k}}^* \varphi_{\vec{k}}^* \rangle_x, \quad \gamma_k = \langle (\varphi^*)^2 \varphi_{-\vec{k}} \varphi_{\vec{k}} \rangle_x,$$
$$\eta_k = |\chi_k|, \gamma_{k,l} = \langle \varphi_k^* \varphi_{-k}^* \varphi_{-l} \varphi_l \rangle_x, \tag{30}$$

and their properties were discussed in more detail in Ref. 19. The only consistent solution preserving hexagonal symmetry is $\chi_k = \chi_c \gamma_k$ where χ_c is a constant independent of $\vec{k}$, and the above equation will be simplified to

TABLE I. Coefficients of the mode expansion for the solid solution.

a_T	g	E_0	E_1	E_3	Δ
−4.6179	−3.43164	0.728715	−0.0022412	−0.00001227	0.6167
−5	−4.96636	1.92669	0.0717767	0.00003881	2.0331
−10	−34.3165	6.29543	0.355908	0.00023872	7.2718
−20	−159.826	13.8477	0.842385	0.00058357	16.3036

$$\mathrm{sgn}(1-\nu)\chi_c\beta_A = \langle \mathrm{sgn}(c^2+\chi_c)\,\eta_k\{[\epsilon_O(\mathbf{k})]^{-1/2} - [\epsilon_A(\mathbf{k})]^{-1/2}\}\rangle_k. \tag{31}$$

For the LK model,[34] $\nu=2$, this leads to $\chi_c\beta_A = \langle \eta_k\{[\epsilon_A(\mathbf{k})]^{-1/2} - [\epsilon_O(\mathbf{k})]^{-1/2}\}\rangle_k$. Finally the set of the minimization equations (using the properties of the lattice functions $\beta_k, \gamma_k, \gamma_{k,l}$) can be derived:

$$\begin{aligned} 0 &= a_T + \beta_A c^2 + 2\langle \beta_k\{[\epsilon_O(\mathbf{k})]^{-1/2} + [\epsilon_A(\mathbf{k})]^{-1/2}\}\rangle_{\mathbf{k}} \\ &\quad + \langle \eta_k\{[\epsilon_O(\mathbf{k})]^{-1/2} - [\epsilon_A(\mathbf{k})]^{-1/2}\}\rangle_{\mathbf{k}}, \\ \chi_c\beta_A &= \langle \eta_k\{[\epsilon_A(\mathbf{k})]^{-1/2} - [\epsilon_O(\mathbf{k})]^{-1/2}\}\rangle_k, \\ \rho_l &= \langle \beta_{l-k}\{[\epsilon_O(\mathbf{k})]^{-1/2} + [\epsilon_A(\mathbf{k})]^{-1/2}\}\rangle_k, \end{aligned} \tag{32}$$

and

$$\epsilon_{O,A}(\mathbf{k}) = a_T + 2\beta_k c^2 + 2\rho_k \pm |(c^2+\chi_c)\gamma_k|. \tag{33}$$

The following formulas can be obtained and used for the calculation of the free energy:

$$\begin{aligned} \langle \rho^2 \rangle &= \langle \beta_{l-k}\{[\epsilon_O(\mathbf{k})]^{-1/2} + [\epsilon_A(\mathbf{k})]^{-1/2}\}\{[\epsilon_O(\mathbf{l})]^{-1/2} \\ &\quad + [\epsilon_A(\mathbf{l})]^{-1/2}\}\rangle_{k,l}, \\ \langle |\chi|^2 \rangle &= \frac{1}{\beta_A}[\langle \eta_k\{[\epsilon_A(\mathbf{k})]^{-1/2} - [\epsilon_O(\mathbf{k})]^{-1/2}\}\rangle_k]^2. \end{aligned} \tag{34}$$

Equation (32) can be solved very easily by using mode expansion and iteration method.[19,34] The spectrum can be written as follows:

$$\epsilon_O(\mathbf{k}) = E(k) + \Delta\eta_k, \quad \epsilon_A(\mathbf{k}) = E(k) - \Delta\eta_k, \tag{35}$$

with $E(k)$ expanded in modes:

$$E(k) = \sum E_n \beta_n(k), \tag{36}$$

where

$$\begin{aligned} \beta_k &= \sum_{n=0}^{\infty} \exp[-2\pi n/\sqrt{3}]\beta_n(k), \\ \beta_n(k) &\equiv \sum_{|\mathbf{X}|^2 = 4\pi n/\sqrt{3}} \exp[i\mathbf{k}\cdot\mathbf{X}], \end{aligned} \tag{37}$$

where $\mathbf{X}$ lies on the lattice which basic "cell" is a primitive cell of the vortex lattice and the integer n determines the distance of a lattice point from the origin. For some integers—for example, $n=2,5,6$—$\beta_n=0$ and the first three nonzero β_n are $\beta_0, \beta_1, \beta_3$. The effective "expansion parameter" is $\exp[-2\pi/\sqrt{3}]=0.0265$ and coefficients decrease exponentially with n.[19] It is quite easy to get a more higher-mode approximation, but it is not necessary as the first few-mode approximation has given us a result with very high precision. As an example, when we retain the first three nonzero β_n expansion approximation, the result can be seen from Table I.

The solution disappears at $a_T=-4.6179$. At this point the solid is no longer a metastable state. $\epsilon_A(\mathbf{k})$ is a gapless mode and $\epsilon_A(\mathbf{k}) \to \mathrm{const}\times\mathbf{k}^2$ for $\mathbf{k}\to 0$ in the large-N model. However, for the perturbative spectrum, $\epsilon_A(\mathbf{k}) \to \mathrm{const}\times\mathbf{k}^4$ for $\mathbf{k}\to 0$.

Using

$$\frac{g_{eff}}{N} = a_T c^2 + \frac{\beta_A}{2}c^4 - \left\langle \rho^2 - \frac{1}{2}|\chi|^2 \right\rangle_x + 2\langle \sqrt{\epsilon_O(\mathbf{k})} + \sqrt{\epsilon_A(\mathbf{k})}\rangle_{\mathbf{k}}, \tag{38}$$

the energy corresponding to the solid solution of the minimization equation (32) is given in Table I. The convergence of the mode expansion is exponential as seen from Table I.

For liquid, we impose the rotation-invariant ansatz with $c^2=0$, $\chi=0$ and obtain the gap equation

$$\rho = \frac{2}{\sqrt{a_T + 2\rho}}, \tag{39}$$

which minimizes the energy

$$g_{liq} = -\rho^2 + 4\sqrt{a_T + 2\rho}. \tag{40}$$

The results for both the liquid and solid free energies are plotted in Fig. 2. The melting point appears at $a_T=-5.15$ where the liquid and solid energies are equal.

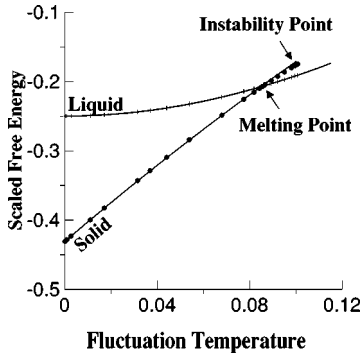

FIG. 2. Free energy of solid (dotted points) and liquid (cross points) of the large-N model as function of the fluctuation temperature $1/|a_T|^{3/2}$. The solid line ends at a point (dot), indicating the loss of metastability.

It is well approximated in the whole region by its low-temperature expansion in powers of $|a_T|^{-3/2}$ [which is proportional to the "fluctuation temperature" T assuming that at low temperatures $a_h \simeq -(1-b)/2$]:

$$\frac{g^{sol}}{a_T^2} = c_M^{sol} + c_1^{sol} T + c_2^{sol} T^2, \ldots, T \equiv |a_T|^{-3/2},$$

$$c_M^{sol} = -\frac{1}{2\beta_A}, \quad c_1^{sol} = 2.84835, \quad c_2^{sol} = -2.54087. \quad (41)$$

The first two terms of this large-N model are the same as for the usual one-component model, while the two-loop correction is different.

Similarly the liquid energy can be expanded, but this time in powers of square of the "fluctuation temperature" T:

$$\frac{g^{liq}}{a_T^2} = c_M^{liq} + c_1^{liq} T + c_2^{liq} T^2, \ldots, T = |a_T|^{-3/2},$$

$$c_M^{liq} = -\frac{1}{4}, \ c_{1,3,\ldots}^{liq} = 0, \ c_2^{liq} = 6, \ c_4^{liq} = -20. \quad (42)$$

Here the first term is the "Madelung energy" of liquid at zero fluctuation temperature. Note that, as in the mean-field approximation to the one-component theory, there is no term linear in T (the harmonic approximation). This means that the specific heat vanishes at zero temperature. Retaining just the Madelung and the harmonic term for solid and liquid we estimate the melting temperature in the linear approximation:

$$T_m = \frac{c_M^{sol} - c_M^{liq}}{c_1^{liq} - c_1^{sol}}. \quad (43)$$

The latent heat in the same approximation is

$$\Delta U = c_M^{sol} - c_M^{liq}. \quad (44)$$

Numerically this melting temperature $T_m = 0.064$ corresponding to $a_T = -6.25$ and the latent heat $\Delta U = 0.18$ should be compared with the exact results: $T_m = 0.086$ ($a_T = -5.15$), $\Delta U = 0.122945$. This shows that the low-temperature expansion of the supercooled liquid free energy gave us quite a sensible result.

In this section we obtain the first-order melting in the mean-field LLL GL model and the large-N LLL GL model. We note that as we show in last section, the GL model or the LLL GL model may not be valid for every low temperature. Thus in reality, the zero-temperature pseudocritical fixed point may not exist, though the LLL GL model does have this pseudocritical fix point at zero temperature. In the mean-field solution of the LLL GL model, the large-N LLL GL model and even the exact solution of the LLL GL model as we will show in the next section, supercooled liquid persists as a metastable state all the way to zero temperature and the superheat vortex solid exists and vanishes at the spinodal line. Based on the fact that the GL LLL model has a zero-temperature fixed point, we could use the Borel-Pade method to calculate the liquid free energy of the LLL GL model at higher temperature (see the next section for details). Therefore we can use this method to calculate the liquid free energy and use it within the validity region of the LLL model. We emphasize that this means that the matching of the (Borel-Pade approximant) liquid to the solid energy at $T=0$ employed in Ref. 14 to improve convergence of the series is not only ineffective,[26] but should lead to an incorrect result. Liquid and solid energies are different in the limit of zero fluctuation temperature in this model.

In a recent experiments, Xiao *et al.* observed the supercooled vortex liquid at very low temperature and the superheat vortex solid which vanishes at spinodal line in 2H-$NbSe_2$ by Ref. 22. They found that the spinodal line is around $a_T = -6$ which is a bit higher than $a_T = -5.5$ in the Gaussian approximation calculation. This small discrepancy could attribute to the fact that Gaussian approximation is not very good for too small a_T.

In atomic liquids, an attractive long-range force is generally present. As a result the supercooled liquid state loses its metastability at an end point (spinodal).[54] Lovett[56] a long time ago argued on general grounds (the stability analysis of approximate set of relations between density correlators) that for certain purely repelling interactions the spinodal point disappears (or, in other words, shifted to zero temperature) and is recovered when the attractive interaction is introduced. The existence of a metastable overcooled liquid down to zero temperature for repelling particles therefore might be quite general.

IV. BOREL-PADE METHOD APPLIED TO THE LLL MODEL: MELTING LINE, MAGNETIZATION, AND SPECIFIC HEAT

A. BP method applied to liquid energy

As we have seen above, within the mean-field approximation of the LLL GL model or the large-N LLL GL model, the liquid branch exhibits a pseudocritical point[55] at $T=0$. It is well known that in the theory of critical phenomena one can obtain an accurate description in the critical region by applying the Borel-Pade method to the perturbation expansion at "weak coupling".[25] In technical terms there exists a renormalization group flow from the weak-coupling fixed point towards the strongly couple one.[24] We therefore start with the (renormalized) weak-coupling (high-temperature or nonideal gas) expansion.

The liquid LLL (scaled) free energy is written as[14]

$$g_{liq} = 4\epsilon^{1/2}[1 + h(x)]. \quad (45)$$

The function h can be expanded as

$$h(x) = \sum c_n x^n, \quad (46)$$

where the "small parameter" $x = \frac{1}{2}\epsilon^{-3/2}$ and ϵ is defined as a solution of the Gaussian gap equation (68). The coefficients c_n can be found in Ref. 27. The consecutive approximants are plotted in Fig. 3 as dashed lines ($T1-T9$, $T0$ being equivalent to the Gaussian mean field). One clearly sees that the series are asymptotic and can be used only at $a_T > -2$. One can improve on the Gaussian variational method by optimizing the variational parameter ϵ at each order instead of fixing it at the first-order calculation. The procedure is rather

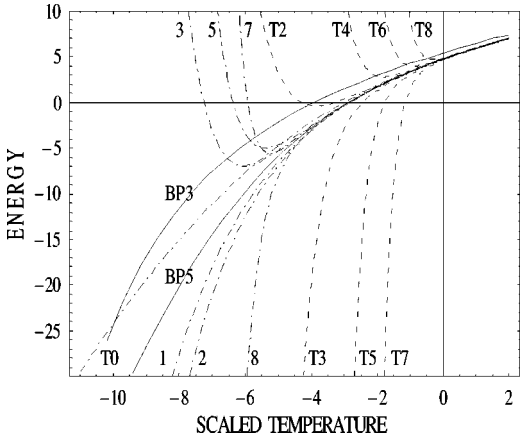

FIG. 3. The BP approximation for the free energy. BP3 and BP5 are the free energy results given by h_3 and h_5. The dashed line T_i is the original perturbative expansion of order i in Ref. 14 and the dot-dashed line i is the optimized expansion of order i.

involved (see Ref. 57). However, the optimized perturbation series is now convergent with radius of convergence about $a_T=-5$ (see dash-dotted lines 1–9 in Fig. 3). Finally we will construct the BP series and compare them with the optimized perturbation series results for $a_T>-5$.

We denote by $h_k(x)$ the $[k,k-1]$ BP transform[25] of $h(x)$ (other BP approximants violate the correct low-temperature asymptotics). The BP transform is defined as

$$h_k = \int_0^\infty \tilde{h}_k(xt)\exp(-t)dt, \tag{47}$$

where $\tilde{h}_k$ is the $[k,k-1]$ Pade transform of $\Sigma_{n=1}^{2k-1} c_n x^n/n!$—namely, a rational function $\Sigma_{i=1}^{k} a_i x^i / \Sigma_{i=1}^{k-1} b_i x^i$ with the same expansion at small x as the original function.

For $k=4$ and $k=5$, the liquid energy converges to required precision (0.1%); see Fig. 3. In this figure only $k=3$ and 5 are shown since $k=4$ practically coincides with the latter. In what follows we will use h_5 as the best available approximation of the liquid branch. The liquid energy completely agrees with the optimized Gaussian expansion results[15] until its radius of convergence at $a_T=-5$. We therefore conclude that $k=5$ is quite good for our purposes.

Since the metastable liquid state exists at all temperatures, one can consider the $T=0$ limit. One finds

$$\frac{g^{liq}(a_T)}{g^{sol}(a_T)} \to 0.964 \tag{48}$$

for $a_T \to -\infty$. For $g^{sol}(a_T)$, the leading term in this limit is $-a_T^2/2\beta_A$, which is the Madelung energy of the solid. The leading term for $g^{liq}(a_T)$ is $-0.964a_T^2/2\beta_A$. Usually the Madelung energy for the solid phase of the point particle system is realized by minimizing the potential energy of the system (the minimum is often obtained by taking the hexagonal lattice for the repulsive system in 2D). In this vortex system, we can have the supercooled liquid down to $a_T \to -\infty$ ($T \to 0$). The leading term for the overcooled liquid energy or the Madelung energy of the liquid is therefore equal to $-0.964a_T^2/2\beta_A$, which is slightly larger than the Madelung energy of the solid. This limit, the "ideal liquid," however, cannot be thought as a minimization of a potential energy.

B. Melting line: Comparison with Monte Carlo simulations and Lindemann criterion

The solid energy calculated perturbatively to two loops is[17,19]

$$g_{sol} = -\frac{a_T^2}{2\beta_A} + 2.848|a_T|^{1/2} + \frac{2.4}{a_T}, \tag{49}$$

where $\beta_A=1.1596$. In Fig. 1 of Ref. 18 we plot the energies of the solid and liquid. They are very close near melting (see the difference on inset of this figure). We find that the melting point (the energy curves of solid and liquid cross at the melting point) is

$$a_T^m = -9.5. \tag{50}$$

The available 3D Monte Carlo simulations[28] unfortunately are not precise enough to provide an accurate melting point since the LLL scaling is violated and one gets values of $a_T^m = -14.5, -13.2, -10.9$ at magnetic fields $(1,2,5)T$ respectively. We found also that the theoretical magnetization calculated by using parameters given by Ref. 28. is in a very good agreement with the Monte Carlo simulation result of Ref. 28. However, the determination of melting temperature needs higher precision, and the sample size ($\sim$100 vortices) used in Ref. 28 may be not large enough to give an accurate determination of the melting temperature (due to boundary effects, LLL scaling will be violated too). The situation in 2D is better since the sample size is much larger. We performed similar calculation for the 2D LLL GL liquid free energy, combined it with the earlier solid energy calculation,[17,19]

$$g_{sol} = -\frac{a_T^2}{2\beta_A} + 2\log\frac{|a_T|}{4\pi^2} - \frac{19.9}{a_T^2} - 2.92, \tag{51}$$

and find that the melting point $a_T^m=-13.2$. It is in good agreement with MC simulations.[30]

Phenomenologically the melting line can be located using the Lindemann criterion or its more refined version using the Debye-Waller factor. The more refined criterion is more appropriate since vortices are not point like. It was found numerically for Yukawa gas[58] that the Debye-Waller factor e^{-2W} (ratio of the structure function at the second Bragg peak at melting to its value at $T=0$) is about 60% at the melting point. Using methods of Ref. 59, one obtains for the 3D LLL GL model at the melting point

$$e^{-2W} = 0.59. \tag{52}$$

C. Fitting of the melting line: Values of the Ginzburg numbers of various superconductors

In this subsection we use the above results to fit experimental melting line of several "fluctuating" superconductors. As an example in Fig. 2 of Ref. 18 we presented the fitting of the melting line of fully oxidized $YBa_2Cu_3O_7$.[6] The melting

lines of two different samples of the optimally doped untwined,[2,40] near T_c ($YBa_2Cu_3O_{7-\delta}$), $DyBa_2Cu_3O_7$,[8] and (K,Ba)BiO_3,[41] are also fitted and the fittings are all extremely well. The results of fittings are given in Table II [To recall our convention, H_{c2} is defined as $T_c dH_{c2}(T)/dT|_{T=T_c}$ rather than $H_{c2}(T=0)$ (often inaccessible)].

Our values for the Ginzburg number of YBCO andDyBCO estimated here are generally lower than the ones commonly believed in the literature. The often-quoted value for YBCO is of order $N_{\rm Gi}=0.01$ (see p. 1134 of commonly used Ref. 10). Direct calculation from Eq. (7) gives $N_{\rm Gi}=0.003$ for $\lambda=1400$ A, $\xi=15$ A, and $\gamma=7$ ($\kappa=93.3$). Note, however, that these values are estimated from measurements at very low temperature. Our values of λ and ξ are fitted to the vortex physics experiments near T_c and extrapolating using the (admittedly questionable) two-liquid model to $T=0$ to give $\lambda=931$ A, $\xi=18.7$ A. Our values of $dH_{c2}(T)/dT$ near T_c are consistent with recent measurement[43] (which is about 2) and smaller than earlier ones. There is no consensus on values of κ measured using the microwave technique at very low temperatures; however, they are also generally smaller than 100 (smaller than 70 at $T=0$ and decreasing with temperature according to Ref. 60 and valued from 50 to 60 according to Ref. 61). This explains the difference of order of magnitude in $N_{\rm Gi}$ between the often-used values and our fitting results (small κ will lead a small $N_{\rm Gi}$ as $N_{\rm Gi}\propto\kappa^4\xi^2T_c^2\gamma^2$). We emphasize that the actual small parameter in the theory is not $N_{\rm Gi}$ but rather $\omega=\sqrt{2{\rm Gi}}\pi^2$ [see Eq. (5)]. Even for Ginzburg number as small as 2×10^{-4} this quantity is 0.2. As a result the effect of thermal fluctuations is important on a significant portion of the phase diagram.

Recently it was found that thermal fluctuation are quite significant even in a low-T_c material (K,Ba)BiO_3. This is despite its lower critical temperature and very small anisotropy (and thereby very small Ginzburg number 5.3×10^{-5}). Since this material is not a "strange metal" or *d*-wave superconductor, its H_{c2} is directly accessible and there is no problem with direct estimate of $N_{\rm Gi}$. However, $\omega=0.1$ for (K,Ba)BiO_3 is not much smaller than that of YBCO. There is therefore no surprise [contrary to a statement in Ref. 41 that fluctuation effects are still experimentally observable in (K,Ba)BiO_3]. In order to be able safely to ignore thermal fluctuations the fluctuation parameter ω should be of order 0.01, in which case $N_{\rm Gi}$ should be smaller than 5×10^{-7}. These are the cases of most low-T_c materials.

D. Magnetization jump at melting

The scaled magnetization (of liquid or solid) is defined by

$$m(a_T)=-\frac{d}{da_T}g(a_T), \tag{53}$$

while the LLL contribution to the magnetization is

$$M_{LLL}=\frac{H_{c2}}{4\pi\kappa^2}\frac{a_h}{a_T}m(a_T). \tag{54}$$

Using expressions, Eq. (49), for solid and Eqs. (45) and (47) for the liquid, the magnetization jump ΔM at the melting point $a_T^m=-9.5$ divided by the magnetization at the melting on the solid side is

$$\frac{\Delta M}{M_s}=\frac{\Delta m}{m_s}=0.018. \tag{55}$$

It is indeed small and is compared on Fig. 2 of Ref. 18 (right inset) with experimental results of fully oxidized $YBa_2Cu_3O_7$ (Ref. 6) (rhombs) and optimally doped untwined $YBa_2Cu_3O_{7-\delta}$ (Ref. 4) (stars). The agreement is quite good. If the HLL contribution is significant (see next section), Eq. (55) is expected to be violated.

E. Specific heat jump at melting

In addition to the δ-function-like spike at melting for specific heat experiments, the experiments also show specific heat jump. The theory allows us to quantitatively estimate it.

The specific heat contribution due to the vortex matter is $C=-T\partial^2/\partial T^2 G(T,H)$. The normalized specific heat is defined as

$$c=\frac{C}{C_{mf}}, \tag{56}$$

where $C_{mf}=H_{c2}^2T/4\pi\kappa^2\beta_A T_c^2$ is the mean-field specific heat of the solid. Substituting the definition of the scaled free energy, Eq. (15), and scaled temperature, Eq. (13), we obtain

$$c=-\frac{16\beta_A}{9t^2}\left(\frac{b\omega}{4\pi\sqrt{2}}\right)^{4/3}g(a_T)+\frac{4\beta_A}{3t^2}(b-1-t)\times\left(\frac{b\omega}{4\pi\sqrt{2}}\right)^{2/3}g'(a_T)-\frac{\beta_A}{9t^2}(2-2b+t)^2g''(a_T). \tag{57}$$

Using our expressions for the energy of the liquid and solid we obtain the following specific heat jump at melting:

TABLE II. Parameters of high T_c superconductors deduced from the melting line.

Material	T_c	H_{c2}	Gi	κ	γ	Reference
$YBCO_{7-\delta}$	93.1	167.5	1.9×10^{-4}	48.5	7.76	2
$YBCO_{7-\delta}$	92.6	190	2×10^{-4}	50	8.3	40
$YBCO_7$	88.2	175.9	7.0×10^{-5}	50	4	6
$DyBCO_{6.7}$	90.1	163	3.2×10^{-5}	33.77	5.3	8
(K,Ba)BiO_3	31	26	5.3×10^{-5}	107	1	41

$$\Delta c = 0.0075\left(\frac{2-2b+t}{t}\right)^2 - 0.20N_{\rm Gi}^{1/3}(b-1-t)\left(\frac{b}{t^2}\right)^{2/3}. \tag{58}$$

Using the parameters of $YBCO_{7-\delta}$ obtained by fitting the melting line, Table II, we compare Eq. (58) with the experimental result of Ref.2 in Fig. 2 of Ref. 18 (right inset). Note that error bars are very large and also that disorder might be important,[51] so that the agreement of the theoretical and experimental result of specific jump is not good as that of the magnetization jump.

V. HIGHER-LANDAU-LEVEL CONTRIBUTIONS: EFFECTIVE LLL MODEL

A. Where is the LLL approximation really valid?

Contributions of HLL are important phenomenologically in two regions of the phase diagram. The first is at a temperature above the mean-field critical temperature $T_c(H)$ inside the liquid phase. The second is far below the melting point deep inside the solid phase.

Naively in the solid phase, when "distance from the mean-field transition line" is smaller than the "inter-Landau-level gap," $1-t-b<2b$, one expects that higher-Landau-level harmonics can be neglected. A more careful examination shows that a weaker condition $1-t-b<12b$ should be used for a validity test of the LLL approximation[44] to calculate the mean-field LLL contributions in a vortex solid. An additional factor of 6 comes from the hexagonal symmetry of the lattice since contributions of higher Landau levels, the first to the fifth HLL, do not appear in the perturbative calculation of the mean-field solution for a vortex solid. In the liquid state the question has been studied by Lawrie[62] using the Hartree-Fock (Gaussian) approximation. The result was that the region of validity is limited, but quite wide; see Fig. 1.

In this section we will incorporate the leading HLL correction using the Gaussian approximation and then compare the theoretical results with experimental magnetization curves.

B. Gaussian approximation in the liquid phase

The free energy density beyond the LLL approximation is

$$G = -\frac{\omega H_{c2}^2}{2\pi\kappa^2 N_{\rm vol}}\log\int \mathcal{D}\psi\mathcal{D}\bar{\psi}\exp\left(-\frac{1}{\omega}\int d^3x\frac{1}{2}|\partial_z\psi|^2 - a_h|\psi|^2+\frac{1}{2}|\psi|^4\right), \tag{59}$$

where $N_{\rm vol}$ denotes volume. In the framework of the Gaussian (Hartree-Fock) approximation the free energy is divided into an optimized quadratic part K and a "small" part V. Then K is chosen in such a way that the Gaussian energy is minimal.[62] The Gaussian energy is a rigorous lower bound on energy. Due to the translational symmetry of the vortex liquid, an arbitrary U(1)-symmetric quadratic part K has only one variational parameter ε:

$$K = \frac{1}{\omega}\int d^3x\left(\frac{1}{2}(|\mathbf{D}\psi|^2 - b|\psi|^2)+\frac{1}{2}|\partial_z\psi|^2+\varepsilon|\psi|^2\right). \tag{60}$$

The small perturbation is therefore

$$V = \frac{1}{\omega}\int d^3x\left[(-a_h-\varepsilon)|\psi|^2+\frac{1}{2}|\psi|^4\right]. \tag{61}$$

The Gaussian energy consists of two parts. The first is the "Tr log" term

$$-\frac{\omega H_{c2}^2}{2\pi\kappa^2{\rm vol}}\log\left[\int\mathcal{D}\psi\exp(-K)\right] = \frac{\omega H_{c2}^2}{2\pi\kappa^2}\frac{b}{\sqrt{2}\pi}\sum_{n=0}^{\infty}\sqrt{nb+\varepsilon}. \tag{62}$$

The second is proportional to the expectation value of v in a solvable model defined by K:

$$\frac{\omega H_{c2}^2}{2\pi\kappa^2}\langle V\rangle = \frac{\omega H_{c2}^2}{2\pi\kappa^2}\left[(-a_h-\varepsilon)\frac{b}{2\sqrt{2}\pi}\sum_{n=0}^{\infty}\frac{1}{\sqrt{nb+\varepsilon}} + \omega\left(\frac{b}{2\sqrt{2}\pi}\sum_{n=0}^{\infty}\frac{1}{\sqrt{nb+\varepsilon}}\right)^2\right]. \tag{63}$$

Both are divergent in the ultraviolet in a sense that at large N the sums diverge. Introducing a UV momentum cutoff which effectively limits the number of Landau levels to $N_f=\Lambda/b-1$, the Tr log term diverges as

$$\frac{1}{\sqrt{2}\pi}b\sum_{n=0}^{\infty}\sqrt{nb+\varepsilon} = \frac{1}{\sqrt{2}\pi}\left[\frac{2}{3}\Lambda^{3/2}+\left(\varepsilon-\frac{b}{2}\right)\Lambda^{1/2}\right]+u(\varepsilon,b), \tag{64}$$

with the last term, the function u, being finite (see Ref. 63 for details). The "bubble" integral diverges logarithmically:

$$\frac{b}{2\sqrt{2}\pi}\sum_{n=0}^{\infty}\frac{1}{\sqrt{nb+\varepsilon}} = \frac{1}{\sqrt{2}\pi}\Lambda^{1/2}+u', \tag{65}$$

where $u'\equiv(\partial/\partial\varepsilon)u(\varepsilon,b)$. Substituting Eq. (64) into the Gaussian energy one obtains (in units of $\omega H_{c2}^2/2\pi\kappa^2$)

$$g_{Gauss} = \frac{1}{\sqrt{2}\pi}\frac{2}{3}\Lambda^{3/2}+\omega\left(\frac{1}{\sqrt{2}\pi}\Lambda^{1/2}\right)^2+\left(-a_h-\frac{b}{2}\right)\frac{1}{\sqrt{2}\pi}\Lambda^{1/2} - a_h u'+2\omega\frac{1}{\sqrt{2}\pi}\Lambda^{1/2}u'-\varepsilon u'+\omega(u')^2+u. \tag{66}$$

The first term does not depend on the parameters of the system and can be ignored (the renormalization of the reference energy density), while the second is ω dependent and indicates that T_c present inside a_h is renormalized. Defining $a_h = a_h^r + 2\omega(1/\sqrt{2}\pi)\Lambda^{1/2}$, the above energy becomes

$$g_{Gauss} = -\omega\left(\frac{1}{\sqrt{2}\pi}\Lambda^{1/2}\right)^2+\left(-a_h^r-\frac{b}{2}\right)\frac{1}{\sqrt{2}\pi}\Lambda^{1/2} - a_h^r u'-\varepsilon u'+\omega(u')^2+u. \tag{67}$$

Thus the temperature T_c and vacuum energy will be renor-

malized. The first two terms in the free energy are divergent and linear in the fluctuation temperature ω; they will not contribute to any physical quantities like magnetization and specific heat. Minimizing the energy, Eq. (67), we get the gap equation

$$\varepsilon = -a_h^r + 2\omega u'. \tag{68}$$

Superscript r will be dropped later on. The function $u(\varepsilon,b)$ can be written in the form

$$u(\varepsilon,b) = \frac{1}{\sqrt{2}\pi} b^{3/2} v\left(\frac{\varepsilon}{b}\right), \tag{69}$$

where

$$v(x) = \sum_{n=0}^{\infty} \left[\sqrt{n+x} - \frac{2}{3}\left(x+n+\frac{1}{2}\right)^{3/2} + \frac{2}{3}\left(x+n-\frac{1}{2}\right)^{3/2} \right] - \frac{2}{3}\left(x-\frac{1}{2}\right)^{3/2}. \tag{70}$$

For the LLL model in the Gaussian approximation, $v(x) = \sqrt{x}$. In the "Prange" limit[64] $N_{\mathrm{Gi}} \to 0$, the free energy is

$$\frac{\omega H_{c2}^2}{2\pi\kappa^2} \frac{1}{\sqrt{2}\pi} b^{3/2} v\left(-\frac{a_h}{b}\right). \tag{71}$$

C. Integration of the HLL modes and the effective LLL model

A method for treating HLL modes is integrating them and obtaining an effective LLL model. The (effective) LLL model is applicable in a surprisingly wide range of fields and temperatures determined by the condition that the relevant excitation energy ε be much smaller than the gap between Landau levels b. Within the mean-field approximation in the liquid ε is a solution of the gap equation (68). For the LLL dominance region, we take a conservative condition $\varepsilon/\varepsilon_c = 1/20$. One observes that, apart from the fields smaller than $H_{LLL} \approx 0.1\ T$ for YBCO, the experimentally observed melting line and its neighborhood are well within the range of applicability of this approximation as shown in Fig. 1.

The effective LLL energy (we will use unit of energy density $H_{c2}^2/2\pi\kappa^2$ in this subsection) functional is defined by

$$g_{eff}[\psi_0] = -\frac{\omega}{N_{\mathrm{vol}}} \log \int \prod_{i=1}^{\infty} \mathcal{D}\psi_i \mathcal{D}\psi_i^* \exp\{-f[\psi_0, \psi_0^*, \psi_i, \psi_i^*,]\}, \tag{72}$$

where ψ_0 is the LLL $N=0$ component field and the rest are denoted by ψ_i. Expanding the functional up to the fourth order in ψ_0 and to the second order in ∂_z one obtains

$$g_{eff}[\psi_0] = \Delta g + \frac{\Delta t}{2}|\psi_0|^2 + \omega f_{LLL}[\psi_0],$$

$$f_{LLL}[\psi_0] = \frac{1}{\omega}\left[\frac{1}{2}|\partial_z\psi_0|^2 - a_h|\psi_0|^2 + \frac{1}{2}|\psi_0|^4\right]. \tag{73}$$

The direct (no ψ_0 dependence) renormalization of energy is

$$\Delta g = -\frac{\omega}{N_{\mathrm{vol}}} \log \int \prod_{i=1}^{\infty} \mathcal{D}\psi_i \mathcal{D}\psi_i^* \exp\{-f_{HLL}[\psi_i]\}, \tag{74}$$

where the HLL energy is

$$f_{HLL} = \frac{1}{\omega}\left[\frac{1}{2}|\partial_z\psi_{HLL}|^2 - a_h|\psi_{HLL}|^2 + \frac{1}{2}|\psi_{HLL}|^4\right], \tag{75}$$

where $\psi_{HLL} = \Sigma_{i=1}^{\infty}\psi_i$. To calculate Δg, we divide the f_{HLL} into

$$K_{HLL} = \frac{1}{\omega}\left(\frac{1}{2}(|\mathbf{D}\psi|^2 - b|\psi|^2) + \frac{1}{2}|\partial_z\psi|^2 + \varepsilon|\psi|^2\right) \tag{76}$$

plus $f_{HLL} - K_{HLL}$. Taking ε as the solution of the gap equation (68), one finds that Δg takes the form

$$\Delta g = g_{Gauss} - g_{LLL} + 2\langle|\psi_0|^2\rangle(\langle|\psi_0|^2\rangle - \langle|\psi|^2\rangle),$$

$$g_{LLL} = -\frac{\omega}{N^{\mathrm{vol}}} \log \int \mathcal{D}\psi_0 \mathcal{D}\psi_0^* \exp\{-f_{LLL}[\psi_0]\}. \tag{77}$$

Here g_{Gauss} is the effective free energy of the full GL obtained in the first subsection of the current section, Eq. (67), and $\langle|\psi|^2\rangle$ is likewise the expectation value of $|\psi|^2$ in the full GL. The quantity g_{LLL} is the effective free energy calculated with variational parameter ε and $\langle|\psi_0|^2\rangle$ is the expectation value in the LLL GL. The consistency (or matching) requirement is

$$g_{eff} = -\frac{\omega}{N_{\mathrm{vol}}} \log \int \mathcal{D}\psi_0 \mathcal{D}\overline{\psi_0} \exp\left\{-\frac{1}{\omega} g_{eff}[\psi_0]\right\}. \tag{78}$$

This condition determines the value of Δt:

$$\Delta t = 4(\langle|\psi|^2\rangle - \langle|\psi_0|^2\rangle) = 4\omega[u'(\varepsilon,b)] - 4\langle|\psi_0|^2\rangle = 4\omega\frac{1}{\sqrt{2}\pi} b^{1/2}\left[v'\left(\frac{\varepsilon}{b}\right) - \frac{1}{2}\sqrt{\frac{b}{\varepsilon}}\right]. \tag{79}$$

For Y BCO, the correction Δt is small. The effective LLL GL approach achieves a simplification by starting from the LLL effective model with T_c and other parameters renormalized to account for the contribution of the HLL modes. This is what we assumed in Secs. III and IV. In particular, this approach is very precise if we calculate the properties along the melting line. For example, the magnetization jump is mostly due to the fluctuation of the LLL modes, and the background effective energy Δg will not contribute anything since it is the same on both sides of the melting line.

D. HLL contribution to the magnetization

Generally when κ is quite large and magnetization can be approximated by

$$M = -\frac{\partial}{\partial H} G(T,H). \tag{80}$$

The HLL correction will be calculated as follows. We numerically solve the gap equation (68) from which $G(T,H)$ can be obtained. Then Eq. (80) is used to calculate the magnetization of the full GL model in the Gaussian approxima-

tion. The HLL correction is thus the magnetization of the full GL model in the Gaussian approximation minus the magnetization of the LLL contribution in the Gaussian approximation. We compare the experiments using the following approximation. While the corrections due to HLL are calculated in the Gaussian approximation, the LLL contribution will be calculated nonperturbatively. The comparison of the theoretical predictions with the experiments for fully oxidized $YBa_2Cu_3O_7$ (Ref. 6), is shown on Fig. 3 of Ref. 18. We used the experimental asymmetry value $\gamma=4$ and values of T_c H_{c2} and N_{Gi} from the fitting of the melting curve (see Table II). The agreement is fair at intermediate magnetic fields, while at low magnetic fields is not good. It is expected that agreement is improved at higher fields. It is not clear whether magnetization (in contrast to magnetization jump at melting) will be strongly influenced by disorder, so at this time it is not possible to consider optimal doped YBCO magnetization curved more quantitatively.

We comment that the theory of the full GL model (higher Landau levels included) beyond the Gaussian approximation is required at low magnetic fields. Indeed experimentally it is often claimed that one can establish the LLL scaling for fields above 3 T for YBCO (see, for example, Ref. 37) as, at low magnetic fields, the HLL contribution will be significant.

VI. SUMMARY

The problem of calculating the fluctuations effects in the framework of the Ginzburg-Landau approach to vortex matter in type-II superconductors is studied in the LLL approximation and basically solved in the LLL limit. The results allow a quantitative description of the melting transition. We provided evidence that in the LLL GL model metastable homogeneous state (the supercooled liquid state) exists down to zero fluctuation temperature and the superheat vortex solid which vanishes at the spinodal line by solving the large-N LLL Ginzburg-Landau model. The recent experiments in 2H-$NbSe_2$ by Xiao *et al.*[22] had been carried out to test the theoretical results based on the LLL GL model and it was found that there indeed exist the supercooled vortex liquid at very low temperature and the superheat vortex solid which vanishes at the spinodal line. Thus the supercooled liquid state can be approached using the methods of the physics of critical phenomena (the Borel-Pade resummation technique). The applicability of the effective lowest-Landau-level model was subsequently discussed and corrections due to higher levels are calculated.

The theory is then applied to quantitatively describe a great variety of experiments (confined to a region not far from T_c) including melting curves of YBCO, DyBCO, and $(K,Ba)BiO_3$, magnetization curves, and discontinuities of various quantities at melting, and it was found that the theoretical results can fit the experimental data quantitatively very well.

ACKNOWLEDGMENTS

We are grateful to E. H. Brandt and X. Hu for numerous discussions, E. Y. Andrei, F. Bouquet, A. Junod, M. Naughton, and T. Nishizaki for providing details of experiments, and Z. Tesanovic and M. Moore for correspondence. We are especially grateful to Y. Rosenfeld for patiently explaining to us his results on one-component plasma. The work of B.R. was supported by NSC of Taiwan Grant No. NSC#93-2112-M-009-023 and the work of D.L. was supported by the Ministry of Science and Technology of China (Grant No. G1999064602) and National Nature Science Foundation (Grant No. 10274030).

[1] E. Zeldov, D. Majer, M. Konczykowski, V. B. Geshkenbein, V. M. Vinokur, and H. Shtrikman, Nature (London) **375**, 373 (1995).

[2] A. Schilling, R. A. Fisher, and G. W. Crabtree, Nature (London) **382**, 791 (1996); A. Schilling, R. A. Fisher, N. E. Phillips, U. Welp, W. K. Kwok, and G. W. Crabtree, Phys. Rev. Lett. **78**, 4833 (1997).

[3] H. Pastoriza, M. F. Goffman, A. Arribêre, and F. de la Cruz, Phys. Rev. Lett. **72**, 2951 (1994); X. Liang, D. A. Bonn, and W. N. Hardy, *ibid.* **76**, 835 (1996).

[4] U. Welp, J. A. Fendrich, W. K. Kwok, G. W. Crabtree, and B. W. Veal, Phys. Rev. Lett. **76**, 4809 (1996).

[5] M. Willemin, A. Schilling, H. Keller, C. Rossel, J. Hofer, U. Welp, W. K. Kwok, R. J. Olsson, and G. W. Crabtree, Phys. Rev. Lett. **81**, 4236 (1998).

[6] K. Shibata, T. Nishizaki, T. Sasaki, and N. Kobayashi, Phys. Rev. B **66**, 214518 (2002).

[7] F. Bouquet, C. Marcenat, E. Steep, R. Calemczuk, W. K. Kwok, U. Welp, G. W. Crabtree, R. A. Fisher, N. E. Phillips, and A. Schilling, Nature (London) **411**, 448 (2001).

[8] M. Roulin, A. Junod, and E. Walker, Science **273**, 1210 (1996); M. Roulin, A. Junod, A. Erb, and E. Walker, J. Low Temp. Phys. **105**, 1099 (1996); B. Revaz, A. Junod, and A. Erb, Phys. Rev. B **58**, 11 153 (1998).

[9] M. Tinkham, *Introduction to Superconductivity* (McGraw-Hill, New York, 1996).

[10] G. Blatter, M. V. Feigel'man, V. B. Geshkenbein, A. I. Larkin, and V. M. Vinokur, Rev. Mod. Phys. **66**, 1125 (1994).

[11] E. Brezin, D. R. Nelson, and A. Thiaville, Phys. Rev. B **31**, 7124 (1985).

[12] Reference 11 assumes a simple ansatz for solutions of the functional RG equations. Newman and Moore [T. J. Newman and M. A. Moore, Phys. Rev. B **54**, 6661 (1996)] performed a more comprehensive analytical and numerical study of the equations relaxing the ansatz and found points. However, upon closer inspection the free energy at these fixed points can be written in the quasimomentum basis [see Eq. (10)] as $\int dz \int d\mathbf{k}\left(-\frac{1}{2}\partial^2/\partial z^2 + \varepsilon\right)\psi^*_{\mathbf{k}}(z)\psi_{\mathbf{k}}(z) + c\,[\psi^*_{\mathbf{k}}(z)\psi_{\mathbf{k}}(z)]^2$. Different momenta in directions xy are decoupled; thus the fixed point is not related to second-order melting. This also explains the appearance of unexpected critical exponents.

[13] G. P. Mikitik and E. H. Brandt, Phys. Rev. B **64**, 184514 (2001);

68, 054509 (2003); J. Kierfeld and V. Vinokur, *ibid.* **61**, R14928 (2000); G. I. Menon, *ibid.* **65**, 104527 (2002).
[14] G. J. Ruggeri and D. J. Thouless, J. Phys. F: Met. Phys. **6**, 2063 (1976).
[15] D. Li and B. Rosenstein, Phys. Rev. Lett. **86**, 3618 (2001).
[16] G. Eilenberger, Phys. Rev. **164**, 628 (1967); K. Maki and H. Takayama, Prog. Theor. Phys. **46**, 1651 (1971).
[17] B. Rosenstein, Phys. Rev. B **60**, 4268 (1999); H. C. Kao, B. Rosenstein, and J. C. Lee, *ibid.* **61**, 12 352 (2000).
[18] D. Li and B. Rosenstein, Phys. Rev. B **65**, 220504(R) (2002).
[19] D. Li and B. Rosenstein, Phys. Rev. B **65**, 024514 (2002).
[20] R. Leote de Carvalho, R. Evans, and Y. Rosenfeld, Phys. Rev. E **59**, 1435 (1999).
[21] B. Tanatar and D. M. Ceperley, Phys. Rev. B **39**, 5005 (1988).
[22] Z. L. Xiao, O. Dogru, E. Y. Andrei, P. Shuk, and M. Greenblatt, Phys. Rev. Lett. **92**, 227004 (2004).
[23] Y. Paltiel, E. Zeldov, Y. N. Myasoedov, H. Shtrikman, S. Bhattacharya, M. J. Higgins, Z. L. Xiao, E. Y. Andrei, P. L. Gammel, and D. J. Bishop, Nature (London) **403**, 398 (2000); Y. Paltiel, E. Zeldov, Y. Myasoedov, M. L. Rappaport, G. Jung, S. Bhattacharya, M. J. Higgins, Z. L. Xiao, E. Y. Andrei, P. L. Gammel, and D. J. Bishop, Phys. Rev. Lett. **85**, 3712 (2000); X. S. Ling, S. R. Park, B. A. McClain, S. M. Choi, D. C. Dender, and J. W. Lynn, *ibid.* **86**, 712 (2001).
[24] D. J. Amit, *Field Theory, the Renormalization Group, and Critical Phenomena* (World Scientific, Singapore, 1984).
[25] G. A. Baker, *Quantitative Theory of Critical Phenomena* (Academic Press, Boston, 1990).
[26] A solvable toy model resembling GL was studied in N. K. Wilkin and M. A. Moore, Phys. Rev. B **47**, 957 (1993). The conclusion was that the BP is unreliable in this model. We however repeated this calculation and found that the correct result is reproduced provided order is high enough (above 100).
[27] S. Hikami, A. Fujita, and A. I. Larkin, Phys. Rev. B **44**, R10400 (1991); E. Brezin, A. Fujita, and S. Hikami, Phys. Rev. Lett. **65**, 1949 (1990); **65**, 2921(E) (1990).
[28] R. Sasik and D. Stroud, Phys. Rev. Lett. **75**, 2582 (1975).
[29] J. Hu and A. H. MacDonald, Phys. Rev. B **56**, 2788 (1997).
[30] Y. Kato and N. Nagaosa, Phys. Rev. B **48**, 7383 (1993); J. Hu and A. H. MacDonald, Phys. Rev. Lett. **71**, 432 (1993); A. E. Koshelev, Phys. Rev. B **56**, 11 201 (1997).
[31] I. F. Herbut and Z. Tesanovic, Phys. Rev. B **49**, 4064 (1994); S. Sengupta *et al.*, Phys. Rev. Lett. **67**, 3444 (1991); G. I. Menon *et al.*, Phys. Rev. B **54**, 16 192 (1996).
[32] I. Affleck and E. Brezin, Nucl. Phys. B **257**, 451 (1985).
[33] M. A. Moore, T. J. Newman, A. J. Bray, and S.-K. Chin, Phys. Rev. B **58**, 9677 (1998).
[34] A. Lopatin and G. Kotliar, Phys. Rev. B **59**, 3879 (1999).
[35] V. Zhuravlev and T. Maniv, Phys. Rev. B **60**, 4277 (1999).
[36] Z. Tesanovic, L. Xing, L. Bulaevskii, Q. Li, and M. Suenaga, Phys. Rev. Lett. **69**, 3563 (1992); Z. Tesanovic and A. V. Andreev, Phys. Rev. B **49**, 4064 (1994).
[37] J. Sok, Ming Xu, Wei Chen, B. J. Suh, J. Gohng, D. K. Finnemore, M. J. Kramer, L. A. Schwartzkopf, and B. Dabrowski, Phys. Rev. B **51**, 6035 (1995); S. W. Pierson and O. T. Walls, *ibid.* **57**, R8143 (1998).
[38] A. E. Koshelev, Phys. Rev. B **50**, 506 (1994).
[39] B. Rosenstein, B. Ya. Shapiro, R. Prozorov, A. Shaulov, and Y. Yeshurun, Phys. Rev. B **63**, 134501 (2001); Y. M. Huh and D. K. Finnemore, *ibid.* **65**, 092506 (2002).
[40] A. Schilling, U. Welp, W. K. Kwok, and G. W. Crabtree, Phys. Rev. B **65**, 054505 (2002).
[41] S. Blanchard, T. Klein, J. Marcus, I. Joumard, A. Sulpice, P. Szabo, P. Samuely, A. G. M. Jansen, and C. Marcenat, Phys. Rev. Lett. **88**, 177201 (2002).
[42] I. Maggio-Aprile, Ch. Renner, A. Erb, E. Walker, and Ø. Fischer, Phys. Rev. Lett. **75**, 2754 (1995); B. Keimer, W. Y. Shih, R. W. Erwin, J. W. Lynn, F. Dogan, and I. A. Aksay, *ibid.* **73**, 3459 (1994).
[43] H. Nakagawa, T. Takamasu, N. Miura, and Y. Enomoto, Physica B **246–247**, 429 (1998).
[44] D. Li and B. Rosenstein, Phys. Rev. B **60**, 9704 (1999).
[45] B. I. Halperin, T. C. Lubensky, and S.-k. Ma, Phys. Rev. Lett. **32**, 292 (1974).
[46] C. J. Lobb, Phys. Rev. B **36**, 3930 (1987).
[47] Z. Tesanovic, Phys. Rev. B **59**, 6449 (1999).
[48] A. Sudbø and A. K. Nguyen, Phys. Rev. B **60**, 15 307 (1999).
[49] W. K. Kwok, R. J. Olsson, G. Karapetrov, and L. M. Paulius, Phys. Rev. Lett. **84**, 3706 (2000).
[50] N. J. Garfield, M. A. Howison, G. Yang, and S. Abel, Physica C **321**, 1 (1999).
[51] D. Li and B. Rosenstein, Phys. Rev. Lett. **90**, 167004 (2003).
[52] T. Giamarchi and P. Le Doussal, Phys. Rev. B **55**, 6577 (1997); S. E. Korshunov, *ibid.* **48**, 3969 (1993).
[53] D. J. Thouless, Phys. Rev. Lett. **34**, 946 (1975); A. J. Bray, Phys. Rev. B **9**, 4752 (1974).
[54] P. G. Debenedetti, *Metastable Liquids: Concepts and Principles* (Princeton University Press Princeton, 1996); P. G. Debenedetti and F. H. Stillinger, Nature (London) **410**, 259 (2001).
[55] A. Compagner, Physica (Amsterdam) **72**, 115 (1974).
[56] R. Lovett, J. Chem. Phys. **66**, 1255 (1977).
[57] D. Li and B. Rosenstein, Phys. Rev. B **65**, 024513 (2002).
[58] M. Stevens and M. Robbins, J. Chem. Phys. **98**, 2319 (1993).
[59] D. Li and B. Rosenstein, Phys. Rev. B **60**, 10 460 (1999).
[60] T. M. Riseman, J. H. Brewer, K. H. Chow, W. N. Hardy, R. F. Kiefl, S. R. Kreitzman, R. Liang, W. A. MacFarlane, P. Mendels, G. D. Morris, J. Rammer, and J. W. Schneider, Phys. Rev. B **52**, 10 569 (1995).
[61] U. Welp, W. K. Kwok, G. W. Crabtree, K. G. Vandervoort, and J. Z. Liu Phys. Rev. Lett. **62**, 1908 (1989).
[62] I. D. Lawrie, Phys. Rev. B **50**, 9456 (1994).
[63] D. Jana, Nucl. Phys. B **473**, 659 (1996); **485**, 747 (1997).
[64] R. E. Prange, Phys. Rev. B **1**, 2349 (1970).